

TECHNICAL ADVANCE

Imaging phosphatidylinositol 4-phosphate dynamics in living plant cells

Joop E.M. Vermeer^{1,2,†}, Julie M. Thole³, Joachim Goedhart¹, Erik Nielsen⁴, Teun Munnik^{2,*} and Theodorus W.J. Gadella Jr¹

¹Department of Molecular Cytology, Centre for Advanced Microscopy, Swammerdam Institute for Life Sciences, University of Amsterdam, Amsterdam, The Netherlands,

²Department of Plant Physiology, Swammerdam Institute for Life Sciences, University of Amsterdam, Amsterdam, The Netherlands,

³Department of Biology, Washington University, One Brookings Drive, St Louis, MO 63130, USA, and

⁴Department of Molecular, Cellular & Developmental Biology, University of Michigan, Ann Arbor, MI 48109, USA

Received 3 April 2008; revised 4 August 2008; accepted 21 August 2008; published online 27 October 2008.

*For correspondence (fax +31 205257924; e-mail T.munnik@uva.nl).

†Present address: Section of Plant Physiology, Swammerdam Institute for Life Sciences, University of Amsterdam, The Netherlands.

Summary

Polyphosphoinositides represent a minor group of phospholipids, accounting for less than 1% of the total. Despite their low abundance, these molecules have been implicated in various signalling and membrane trafficking events. Phosphatidylinositol 4-phosphate (PtdIns4P) is the most abundant polyphosphoinositide. ³²Pi-labelling studies have shown that the turnover of PtdIns4P is rapid, but little is known about where in the cell or plant this occurs. Here, we describe the use of a lipid biosensor that monitors PtdIns4P dynamics in living plant cells. The biosensor consists of a fusion between a fluorescent protein and a lipid-binding domain that specifically binds PtdIns4P, i.e. the pleckstrin homology domain of the human protein phosphatidylinositol-4-phosphate adaptor protein-1 (FAPP1). YFP-PH_{FAPP1} was expressed in four plant systems: transiently in cowpea protoplasts, and stably in tobacco BY-2 cells, *Medicago truncatula* roots and *Arabidopsis thaliana* seedlings. All systems allowed YFP-PH_{FAPP1} expression without detrimental effects. Two distinct fluorescence patterns were observed: labelling of motile punctate structures and the plasma membrane. Co-expression studies with organelle markers revealed strong co-labelling with the Golgi marker STtmd-CFP, but not with the endocytic/pre-vacuolar marker GFP-AtRABF2b. Co-expression with the PtdIns3P biosensor YFP-2 × FYVE revealed totally different localization patterns. During cell division, YFP-PH_{FAPP1} showed strong labelling of the cell plate, but PtdIns3P was completely absent from the newly formed cell membrane. In root hairs of *M. truncatula* and *A. thaliana*, a clear PtdIns4P gradient was apparent in the plasma membrane, with the highest concentration in the tip. This only occurred in growing root hairs, indicating a role for PtdIns4P in tip growth.

Keywords: phosphoinositides, GFP, membrane trafficking, microscopy, lipid binding domain.

Introduction

Phosphatidylinositolmonophosphate (PtdInsP) is a minor lipid present in all eukaryotic membranes, accounting for less than 1% of total phospholipids (Meijer and Munnik, 2003; Munnik *et al.*, 1998). In nature, three isomers occur, which differ in the position of the phosphate group on the D-myoinositol ring, i.e. PtdIns3P, PtdIns4P and PtdIns5P, which are formed by specific kinases and phosphatases

(Mueller-Roeber and Pical, 2002; Meijer and Munnik, 2003; Shisheva, 2008).

PtdIns5P, the last isomer that was discovered, accounts for approximately 15% of the ³²P-labelled PtdInsP pool in plants, and has been implicated in the response to osmotic stress (Meijer *et al.*, 2001). Similar amounts are present in mammalian cells, where it has been implicated in host-

pathogen interactions and apoptosis (Gozani *et al.*, 2003; Pendaries *et al.*, 2006). PtdIns3P accounts for approximately 10% of a plant's ^{32}P -labelled PtdInsP pool (Meijer *et al.*, 2001; Munnik *et al.*, 1994a,b). In yeast and mammalian cells, PtdIns3P is an important regulator of endocytosis and vesicular trafficking (Corvera *et al.*, 1999; Simonsen *et al.*, 2001; Stenmark and Gillooly, 2001), and this is probably also the case for plants (Kim *et al.*, 2001; Vermeer *et al.*, 2006). PtdIns4P is the most abundant isomer, making up approximately 80% of the plant PtdInsP pool (Meijer and Munnik, 2003; Meijer *et al.*, 2001; Munnik *et al.*, 1994b). In addition to being important for phospholipase C (PLC) signalling, as a substrate itself, or as a precursor for PtdIns(4,5) P_2 , PtdIns4P has also been recognized as an important signalling molecule involved in membrane trafficking and cytoskeletal organization as known from mammalian and yeast studies (Audhya and Emr, 2002; Audhya *et al.*, 2000; Balla *et al.*, 2002, 2005).

In plants, functional data on PtdIns4P are still very limited. In the genome of Arabidopsis, 12 putative phosphoinositide (PI) 4-kinases have been predicted, classified as PI4K α 1–2, β 1–2 and γ 1–8 (Mueller-Roeber and Pical, 2002). So far, kinase activity has only been established for PI4K α 1 and β 1. Moreover, PI4K γ 1–8 are likely to represent a novel protein kinase family (Galvão *et al.*, 2008). Over-expression of a truncated version of *AtPI4K β 1* in Arabidopsis protoplasts was shown to affect vesicle trafficking (Kim *et al.*, 2001). Knocking out both *AtPI4K β 1* and β 2 genes in Arabidopsis resulted in root hairs with disrupted polarity (Preuss *et al.*, 2006). Moreover, a mutant with a defect in root hair development was recently discovered to carry a mutation in a PtdIns4P phosphatase (Thole *et al.*, 2008). Together, these data indicate an important role for PtdIns4P in root hair growth.

In vitro, PI 4-kinase activity has been detected in several cellular fractions, including cytosol, plasma membrane, microsomal membranes and actin-enriched fractions (Okpodu *et al.*, 1995; Stevenson *et al.*, 1998; Stevenson-Paulik *et al.*, 2003; Yang *et al.*, 1993). GFP fusions in insect cells revealed that GFP-AtPI4K α 1 was localized to the peri-nuclear region, whereas GFP-AtPI4K β 1 was localized in undefined punctate structures (Stevenson-Paulik *et al.*, 2003). More recently, AtPI4K β 1 was shown to localize to the tip of growing root hairs (Preuss *et al.*, 2006). Where PtdIns4P resides is largely unknown.

In this study, we have used a fusion between a fluorescent protein and the PtdIns4P-specific pleckstrin homology domain of human phosphatidylinositol-4-phosphate adaptor protein-1 (HsFAPP1) (Dowler *et al.*, 2000; Levine and Munro, 2002) to monitor PtdIns4P dynamics in living plant cells. Four commonly used model systems were validated: transient expression in cowpea protoplasts, and stable expression in tobacco BY-2 cells, *Medicago truncatula* roots and *Arabidopsis thaliana* seedlings. All four systems

allowed PtdIns4P visualization without noticeable effects on cell growth and development. Two PtdIns4P pools could be distinguished: one at the plasma membrane and one at the Golgi. During cell division in BY-2 cell, and polarized tip growth in *Medicago* and Arabidopsis root hairs, interesting observations were made that suggest PtdIns4P-specific functions that are independent of the PtdIns(4,5) P_2 and PLC signalling paradigm.

Results

YFP-PH_{FAPP1} expression in cowpea protoplasts

In yeast and mammalian cells, GFP-PH_{FAPP1} has been shown to function as a robust *in vivo* marker for PtdIns4P (Balla *et al.*, 2005; Dowler *et al.*, 2000; Levine and Munro, 2002). To investigate the use of this biosensor in living plant cells, we re-cloned it into a plant vector and expressed it transiently in cowpea protoplasts under the control of a 35 S promoter. As shown in Figure 1(a–d), YFP-PH_{FAPP1} typically labelled the plasma membrane and certain motile punctate structures. These structures were approximately $0.73 \pm 0.1 \mu\text{m}$ in size ($n = 50$), and their motility was inhibited by latrunculin A but not by oryzalin, indicating that movement was dependent on the actin cytoskeleton and not microtubules (data not shown). To determine the identity of the motile structures, protoplasts were co-transfected with the endosomal/pre-vacuolar marker GFP-AtRABF2b (Lee *et al.*, 2004; Ueda *et al.*, 2004) or the trans-Golgi marker STtmd-CFP (Boevink *et al.*, 1998). YFP-PH_{FAPP1} fluorescence showed a strong overlap with STtmd-CFP (Figure 1e–h) but not with GFP-AtRABF2b (Figure 1i–l), indicating that the YFP-PH_{FAPP1}-labelled structures were Golgi stacks.

Mutational analysis of YFP-PH_{FAPP1}

To investigate whether the localization of YFP-PH_{FAPP1} was dependent on PtdIns4P, two point mutations were introduced (i.e. K7E and R18L) that are known to abolish PtdIns4P binding (Godi *et al.*, 2004; Levine and Munro, 2002; Park *et al.*, 2003). When expressed in cowpea protoplasts, YFP-PH_{FAPP1-K7E} and YFP-PH_{FAPP1-R18L} no longer labelled the plasma membrane (Figure 1m,q). YFP-PH_{FAPP1-R18L} was still faintly localized to the Golgi stacks but YFP-PH_{FAPP1-K7E} was mainly cytosolic and partly nuclear (compare Figure 1m,n and Figure 1q,r). The large increase in cytosolic localization indicates a loss of binding of the sensor to PtdIns4P-containing membranes. Labelling of the nucleus is probably due to diffusion of the sensor into the nucleus. When these constructs were expressed in mammalian HeLa cells, similar residual Golgi localization of YFP-PH_{FAPP1-R18L} was observed, but YFP-PH_{FAPP1-K7E} was again completely cytosolic (Figure S1a–c).

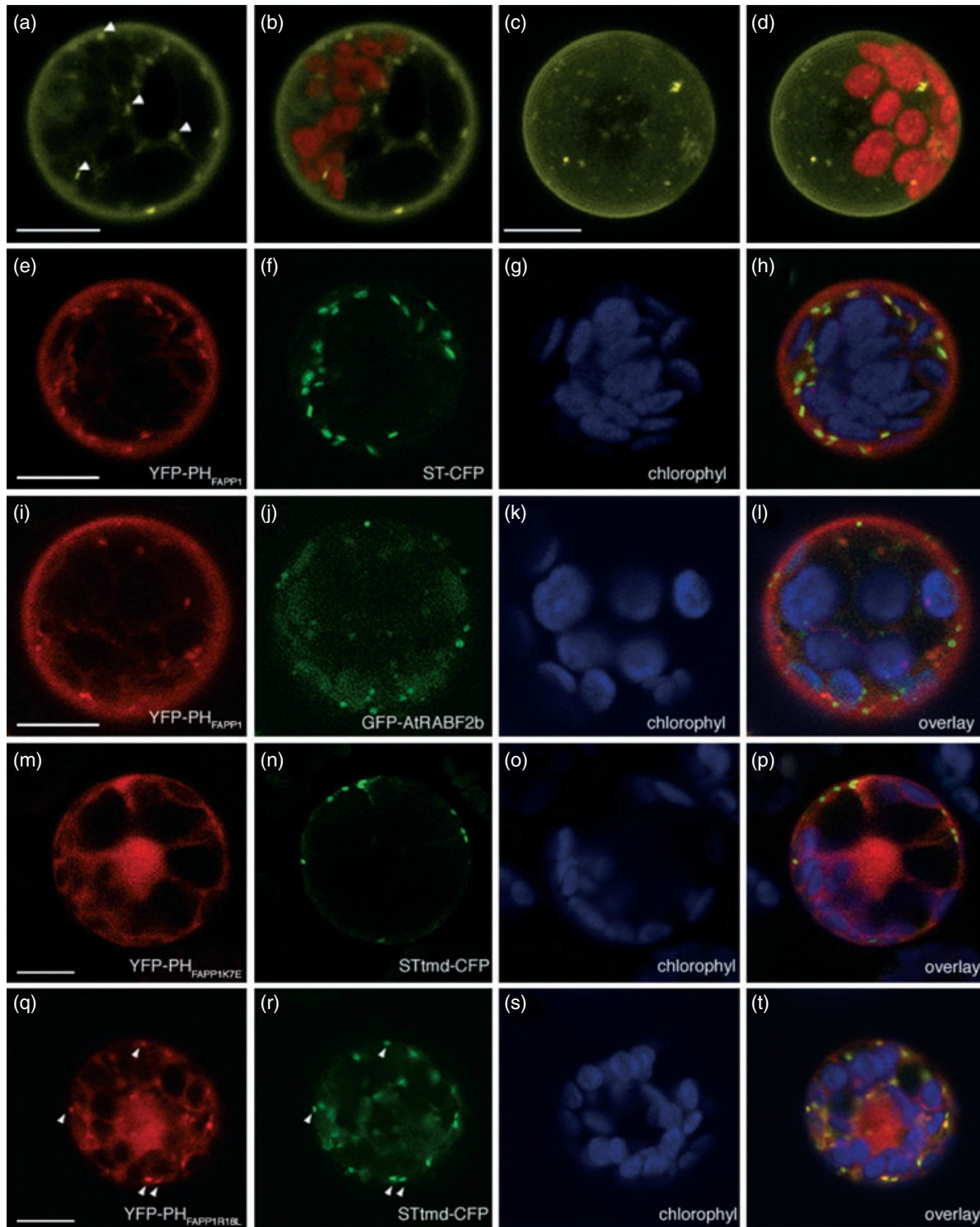


Figure 1. Expression of YFP-PH_{FAPP1} in cowpea protoplasts and identification of YFP-PH_{FAPP1}-labelled punctate structures. Confocal micrographs of cowpea protoplasts expressing YFP-PH_{FAPP1} (a–d), YFP-PH_{FAPP1} plus STtmd-CFP (e–h), YFP-PH_{FAPP1} plus GFP-AtRABF2b (i–l), YFP-PH_{FAPP1-K7E} plus STtmd-CFP (m–p), and YFP-PH_{FAPP1-R18L} plus STtmd-CFP (q–t). (a, b, e–t) Median confocal sections of a protoplast expressing YFP-PH_{FAPP1}. (c, d) Maximum projection of an image stack of the same protoplast. Arrowheads in (a) indicate punctate structures labelled by YFP-PH_{FAPP1}, arrowheads in (q) show residual Golgi labelling by YFP-PH_{FAPP1-R18L}. YFP fluorescence is shown in yellow (a–d) or red (e, i, m, q), GFP and CFP fluorescence are shown in green (f, j, n, r), and chlorophyll is shown in red (b, d) or blue (g, k, o, s). The images are representative of at least five independent transfections. Overlay of fluorescence is shown in (b, d, h, j, l, p, t). Scale bars = 10 μm.

Localization of PtdIns4P in stably transformed BY-2 cells

While the advantage of a transient protoplast system is that GFP constructs can be quickly assessed, a limitation is that protoplasts are often physiologically stressed by the procedure of making them and/or by the sudden over-expression of a recombinant protein (Vermeer, 2006). To further investigate the expression pattern of YFP-PH_{FAPP1}, stably transformed tobacco BY-2 cells were generated.

Cells stably expressing YFP-PH_{FAPP1} or mRFP-PH_{FAPP1} grew and appeared normal, indistinguishable from wild-type cells (data not shown). Fluorescence was mostly associated with the cell periphery and motile punctate structures (Figure 2a–d, Figure S2 and Movie S1). A faint cytoplasmic and nucleoplasmic background was also observed, probably reflecting unbound YFP-PH_{FAPP1} (Figure 2a–d, Figure S2 and Movie S1). Mannitol-induced plasmolysis and co-labelling with the endocytic tracer FM4-64 confirmed that the PtdIns4P biosensor did indeed label the plasma membrane

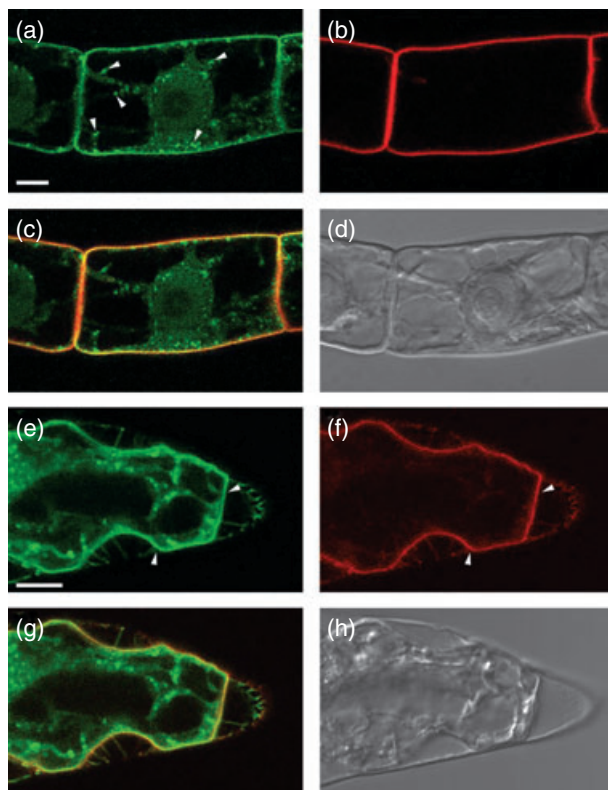


Figure 2. YFP-PH_{FAPP1} detects multiple PtdIns4P pools in tobacco BY-2 cells. YFP-PH_{FAPP1} localizes to the plasma membrane and punctate structures. (a–h) Cells stably expressing YFP-PH_{FAPP1} were co-stained with 2 μ M FM4-64 for 1 min to label the plasma membrane in the control (a–d) or treated with 250 mM mannitol to induce plasmolysis (e–h). Arrowheads in (a) show YFP-PH_{FAPP1}-labelled punctate structures; arrowheads in (e) indicate YFP-PH_{FAPP1}-labelled plasmolysed plasma membrane. YFP fluorescence is shown in green (a, e), FM4-64 fluorescence in red (b, f) and DIC image in grey. (c, g) Merged images. Images are representative of multiple experiments ($n > 5$). Scale bar = 10 μ m.

(Figure 2a–h). Following endocytic uptake of FM4-64 over 20 min using time-lapse confocal microscopy revealed hardly any co-labelling between FM4-64 and YFP-PH_{FAPP1} (Figure 3 and Movie S2). After 20 min, compartments started to appear closer to each other and sometimes even overlapped (arrowheads in Figure 3i–k). This could be the Golgi, as Bolte *et al.* (2004) reported that Golgi membranes can be labelled with FM4-64 within 30 min. Nonetheless, these results clearly indicate that PtdIns4P is absent from early endocytic compartments. To confirm that YFP-PH_{FAPP1} also detected a PtdIns4P pool in the Golgi, co-expression studies with STmd-CFP were performed. As shown in Figure 4 and Movie S3, strong co-labelling between mRFP-PH_{FAPP1} and STmd-CFP was found.

PtdIns4P and PtdIns3P in BY-2 cells

The difference between PtdIns3P and PtdIns4P is the phosphate group on the 3- or 4-position of the *D*-myo-inositol ring. PtdIns3P has previously been imaged using the biosensor YFP-2 \times FYVE (Vermeer *et al.*, 2006; Voigt *et al.*, 2005). To investigate whether there is any overlap between PtdIns3P and PtdIns4P pools, stably transformed BY-2 cells expressing both biosensors were generated.

mRFP-PH_{FAPP1} was present on the plasma membrane and Golgi structures, but YFP-2 \times FYVE clearly labelled a different population of membrane structures (Figure 5 and Movie S4) that were previously identified as late endosomal compartments (Vermeer *et al.*, 2006; Voigt *et al.*, 2005). Frequently, however, we observed these pools in close proximity to each other (Figure 5h).

Are phenylarsine oxide and wortmannin PI 4-kinase inhibitors in plant cells?

In mammalian cells, phenylarsine oxide (PAO) has been shown to decrease PtdIns4P levels, presumably through inhibition of a PI 4-kinase activity (Wiedemann *et al.*, 1996). Wortmannin is widely used as PI 3-kinase inhibitor (Arcaro and Wymann, 1993; Stephens *et al.*, 1994), but has also been reported to affect PtdIns4P levels in both mammalian and plant cells (Balla *et al.*, 2005; Matsuoka *et al.*, 1995). Recently, higher concentrations of wortmannin were found to inhibit isoform-specific (type III) PI 4-kinases, which have kinase domains that closely resemble those of PI 3-kinases (Krinke *et al.*, 2007). Having the BY-2 cells express both biosensors allowed us investigate the effect of these inhibitors on PtdIns3P and PtdIns4P pools simultaneously.

Within 20 min after adding 20 μ M PAO, most of the membrane-localized mRFP-PH_{FAPP1} was lost and reappeared in the cytoplasm and nucleus, indicating unbound mRFP-PH_{FAPP1}. In contrast, the fluorescence pattern of YFP-2 \times FYVE hardly changed (Figure 6a–d and Movie S5). The cyto-architecture of the cells did change: cytoplasmic

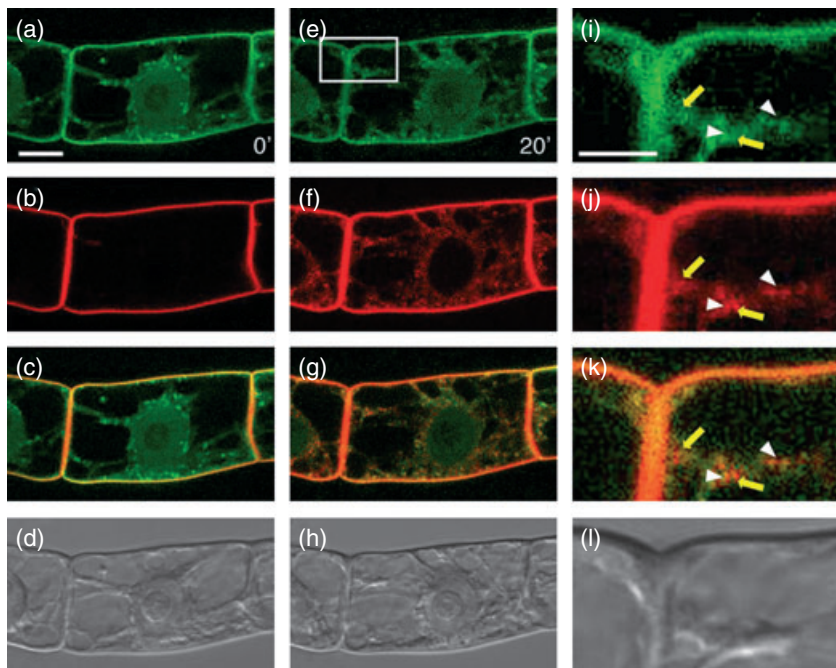


Figure 3. YFP-PH_{FAPP1}-labelled structures are not early endocytic structures.

Cells expressing YFP-PH_{FAPP1} were imaged immediately after addition of 2 μM FM4-64 or after 20 min. Partial co-labelling with FM4-64-positive compartments is only visible after 20 min (i, k).

(i-l) Close-ups of the boxed area in (e) showing compartments with only FM4-64 (yellow arrows) and partial overlap between YFP-PH_{FAPP1} and FM4-64-labelled compartments (arrowheads). YFP fluorescence is shown in green (a, e, i), FM4-64 fluorescence is shown in red (b, f, j), and DIC is shown in grey (d, h, l).

(c, g, k) Merged images. Results are representative of three independent experiments. Scale bar = 10 μm (a-h) or 5 μm (i-l).

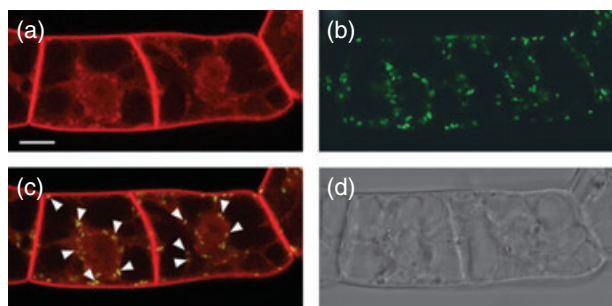


Figure 4. mRFP-PH_{FAPP1}-labelled punctate structures are Golgi membranes. Tobacco BY-2 cells expressing mRFP-PH_{FAPP1} and the Golgi marker STtmd-CFP show clear co-localization at Golgi stacks.

(a) mRFP-PH_{FAPP1} fluorescence (red);
 (b) STtmd-CFP fluorescence (green);
 (c) overlay;
 (d) DIC image. Arrowheads indicate several mRFP-PH_{FAPP1}-labelled Golgi stacks. Scale bar = 10 μm.

strands vanished and large vacuoles appeared (Figure 6a-d). This was even more evident after 45 min (Figure 6e-h). Confocal time-lapse imaging revealed that cytoplasmic streaming and the movement of YFP-2 × FYVE-labelled vesicles was greatly impaired (Movie S6). As treatment with 20 μM PAO had such a strong effect on the mRFP-PH_{FAPP1} localization, the effect of PAO on PtdIns4P levels was investigated further. BY-2 cells were pre-labelled for 5 min with ³²P_i, and then treated with either 20 μM PAO for 15, 30 and 45 min or 0.05% v/v DMSO as a control. Lipids were subsequently extracted, separated by TLC, and quantified by phosphoimaging. In contrast to the strong effect of PAO on

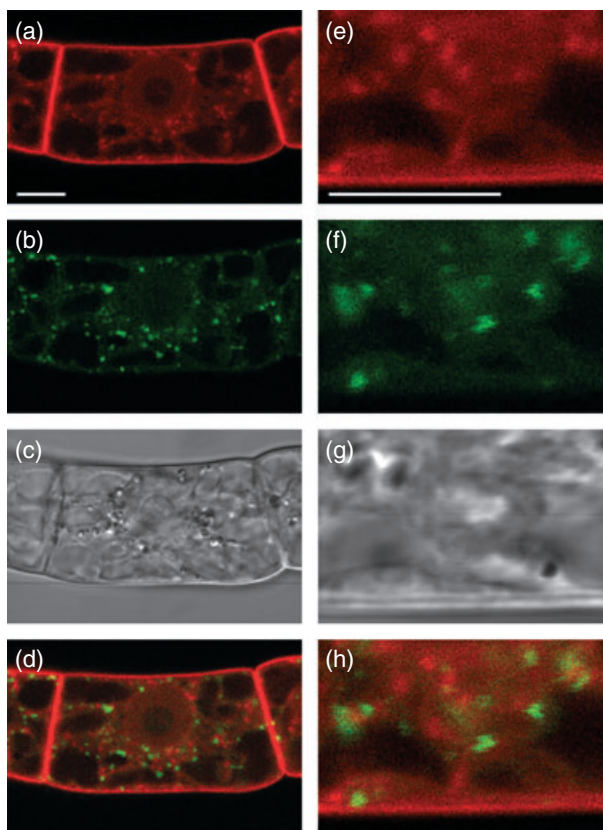


Figure 5. Simultaneous imaging of PtdIns3P and PtdIns4P.

(a-d) Tobacco BY-2 cells stably expressing YFP-2 × FYVE and mRFP-PH_{FAPP1}. (e-h) Close-ups of the same cell showing no overlap between fluorescent signals. (a, e) mRFP fluorescence; (b, f) YFP fluorescence; (c, g) DIC image; (d, h) overlay. Scale bar = 10 μm.

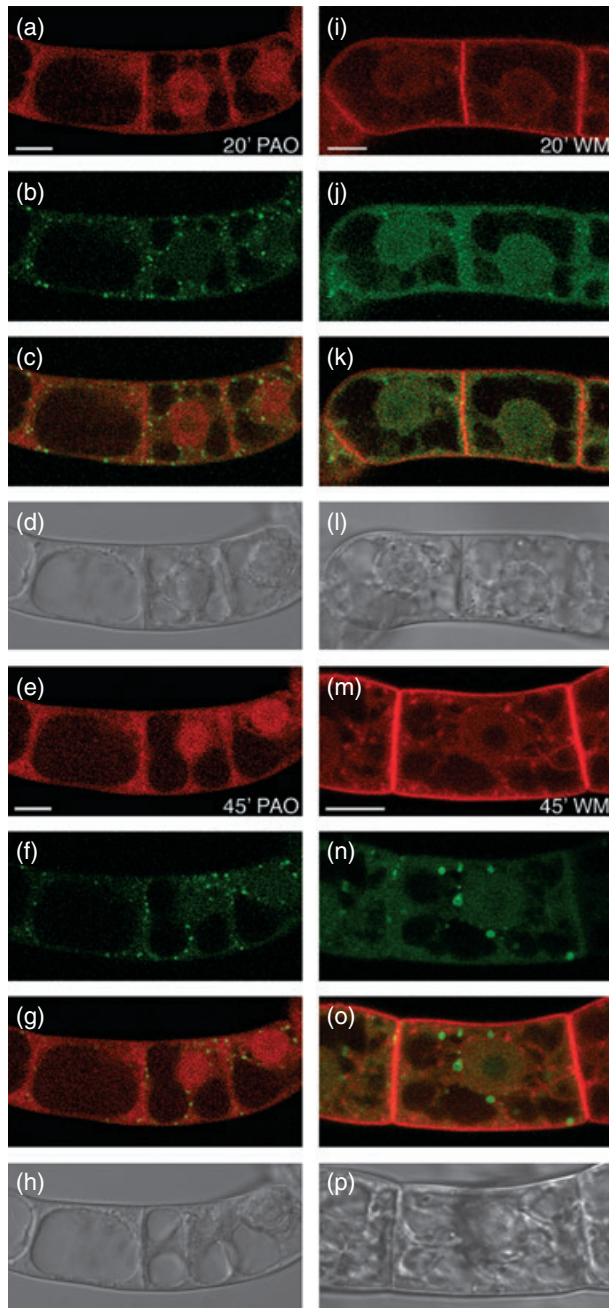


Figure 6. Effect of phenylarsine oxide (PAO) and wortmannin (WM) on the localization of mRFP-PH_{FAPP1} and YFP-2 × FYVE. BY-2 cells stably expressing both biosensors were treated with 20 μM PAO (a–h) or 10 μM WM (i–p) for 20 min (a–d, i–l) or 45 min (e–h, m–p). mRFP fluorescence in red (a, e, i, m); YFP fluorescence in green (b, f, j, n); merged image (c, g, k, o); DIC image in grey (d, h, l, p). Experiments were repeated three times. Scale bar = 10 μm.

mRFP-PH_{FAPP1} localization, no effect was found on ³²P-PtdInsP levels (Figure S3). We do not understand why this is, and this is discussed further below.

Treatment of the cells with 10 μM wortmannin resulted in a complete loss of YFP-2 × FYVE labelling of the punctate

structures within 20 min and a subsequent increase of labelling in the cytosol, but the localization of mRFP-PH_{FAPP1} remained unaffected (Figure 6i–l and Movie S7). After 45 min, the fluorescence pattern of mRFP-PH_{FAPP1} was still not affected, while YFP-2 × FYVE started to appear on larger membrane structures (Figure 6m–p and Movie S8) (Vermeer *et al.*, 2006). In contrast to PAO, wortmannin hardly affected the cyto-architecture of the cells (compare Figure 6h and Figure 6p). When a threefold higher wortmannin concentration (i.e. 30 μM) was used, no alterations in the above-described patterns were observed (Figure S4).

PtdIns4P dynamics during cytokinesis in BY-2 cells

In dividing BY-2 cells, we previously found that YFP-2 × FYVE was predominantly present on vesicular structures in the vicinity of the expanding cell plate, but was never actually found on the newly formed cell membrane (Vermeer *et al.*, 2006). Interestingly, monitoring both sensors simultaneously revealed that mRFP-PH_{FAPP1} labelled the growing cell plate right from the start (Figure 7a,b and Movie S9). When YFP-PH_{FAPP1} cells were co-labelled with the endosomal tracer FM4-64 (2 μM), FM4-64 was found to label the cell plate just before YFP-PH_{FAPP1} fluorescence was detected (Figure 7c,d and Movie S10). This implies that *PtdIns4P* appears just after the cell plate has been initiated, which might reflect its role in cell-plate expansion. The results demonstrate beautifully the differential roles that the *PtdInsP* isomers can play.

Localization of YFP-PH_{FAPP1} and YFP-2 × FYVE in *Medicago truncatula* root hairs

Next, we tested the expression of both biosensors in the stably transformed root system of the model legume *Medicago truncatula* (Boisson-Dernier *et al.*, 2001; Mirabella *et al.*, 2004). As shown in Figure 8(a–m), YFP-PH_{FAPP1} clearly labelled the plasma membrane and punctate structures, the latter probably again being Golgi stacks. Interestingly, in emerging and growing root hairs, a clear tip-localized gradient of YFP-PH_{FAPP1} at the plasma membrane was observed, which was absent in root hairs that had stopped growing (compare Figure 8e,g,i–k with Figure 8m). Control roots transformed with the mutated mRFP-PH_{FAPP1-K7E} only showed cytosolic fluorescence (Figure 8o–t). In comparison, YFP-2 × FYVE labelled numerous vesicular structures and vacuolar membranes, but was not enriched in the tip area (Figure 8u–x). These results indicate a specific role for *PtdIns4P* in root hair growth.

Localization of YFP-PH_{FAPP1} in *Arabidopsis* seedlings

To image *PtdIns4P* dynamics in whole plants, stably transformed *Arabidopsis thaliana* lines were generated.

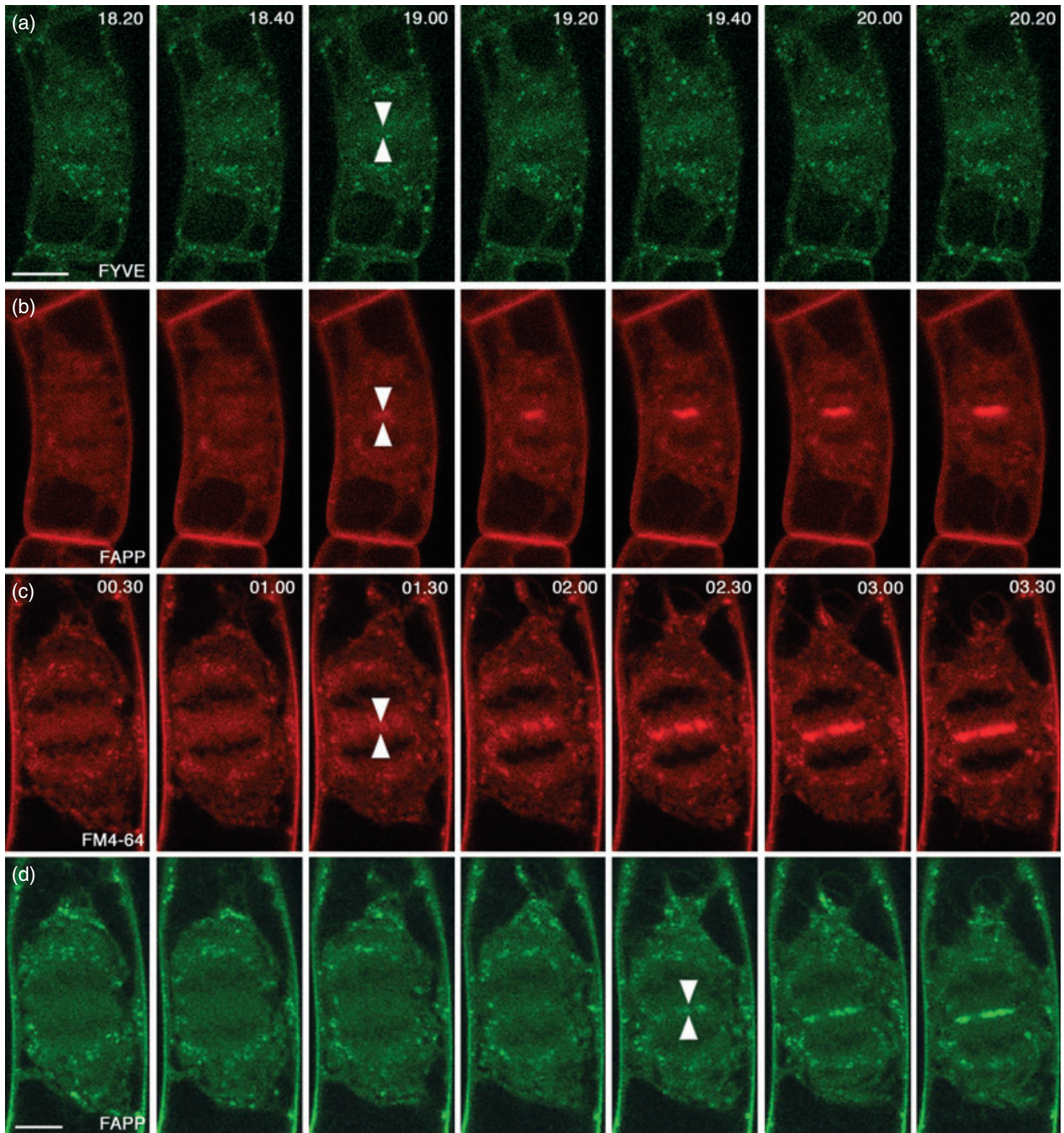


Figure 7. PtdIns3P and PtdIns4P dynamics during cell division in BY-2 cells. (a, b) Confocal time-lapse images of a dividing BY-2 cell co-expressing mRFP-PH_{FAPP1} (red) and YFP-2 × FYVE (green). mRFP-PH_{FAPP1} labels the cell plate (double arrow heads), but YFP-2 × FYVE fluorescence appears to be completely absent. (c, d) Confocal time-lapse images of a dividing BY-2 cell expressing YFP-PH_{FAPP1} (green) co-labelled with 2 μM FM4-64 (red). The time series shows that FM4-64 accumulates at the cell plate prior to YFP-PH_{FAPP1} fluorescence. Time is indicated in minutes corresponding to Movies S9 and S10. For both experiments, at least 3–5 cell divisions were followed. Scale bar = 10 μm.

Homozygous T₃ lines, expressing YFP-PH_{FAPP1} under the control of the 35 S promoter, grew normally and were indistinguishable from wild-type (Col-0) or mRFP-PH_{FAPP1-K7E}-transformed plants (not shown). Seedlings from at least three independent transformed lines expressing YFP-

PH_{FAPP1} all revealed similar fluorescence patterns to those described above for the other model systems, i.e. strong labelling of the plasma membrane, with occasionally some punctate structures moving through the cytosol (Figure 9a,d). Plasma membrane labelling was seen in all cell

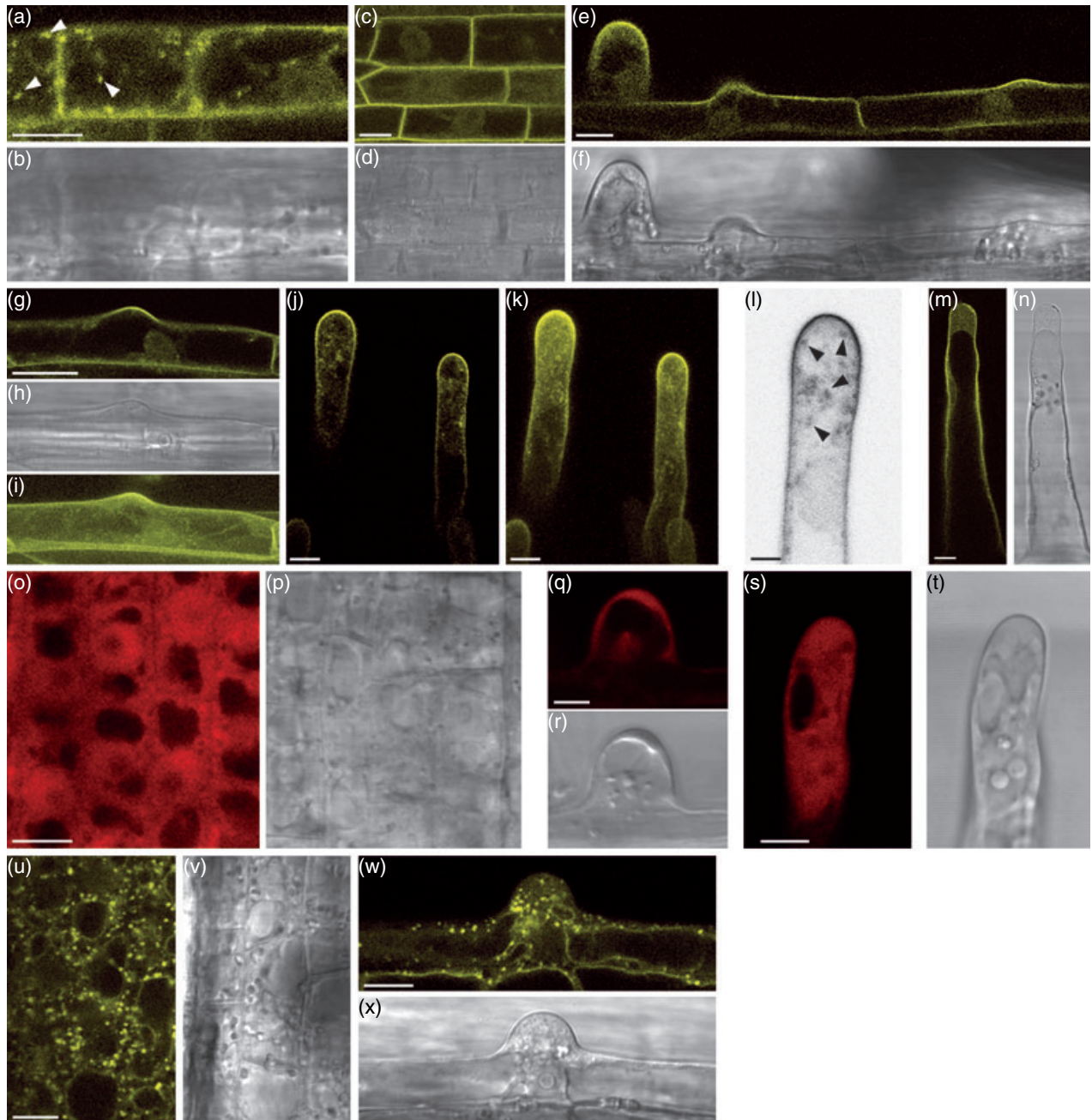


Figure 8. Expression of YFP-PH_{FAPP1}, mRFP-PH_{FAPP1K7E} and YFP-2 × FYVE in *M. truncatula* roots.

Roots were transformed with YFP-PH_{FAPP1} (a–n), mRFP-PH_{FAPP1K7E} (o–t) or YFP-2 × FYVE (q–x).

(a–d) Root epidermal cells, (e–i) emerging, (j–l) growing, and (m, n) non-growing root hairs showing YFP-PH_{FAPP1} fluorescence localized to the plasma membrane and punctate structures in the cytosol (arrowheads).

(i) Maximal projection of an image stack taken from an emerging root hair in (g); (k) maximal projection of an image stack taken from root hairs in (j).

(l) Inverted image of growing root hair showing the tip-focused gradient of fluorescence in root hair from (j). (o, p) Root epidermal cells, (q, r) emerging root hair, and (k, l) growing root hairs expressing mRFP-PH_{FAPP1K7E} displaying cytosolic fluorescence.

(u, v) Root epidermal cells and emerging root hairs expressing YFP-2 × FYVE. (a, c, e, g, i–k, m, u, w) YFP fluorescence in yellow; (o, q, s) mRFP fluorescence in red; (b, d, f, h, n, p, r, t, v, x) DIC images. Images are representative of multiple transformed roots ($n = 5$). Scale bars = 10 μm.

types, including leaf epidermal and guard cells (Figure 9s,u). Seedlings expressing mRFP-PH_{FAPP1K7E} only showed fluorescence in the cytosol (Figure S5). In growing root hairs, a

tip-localized PtdIns4P gradient at the plasma membrane was again observed, which was always lacking in non-growing root hairs (Figure 10g,k and Figures S6 and S7).

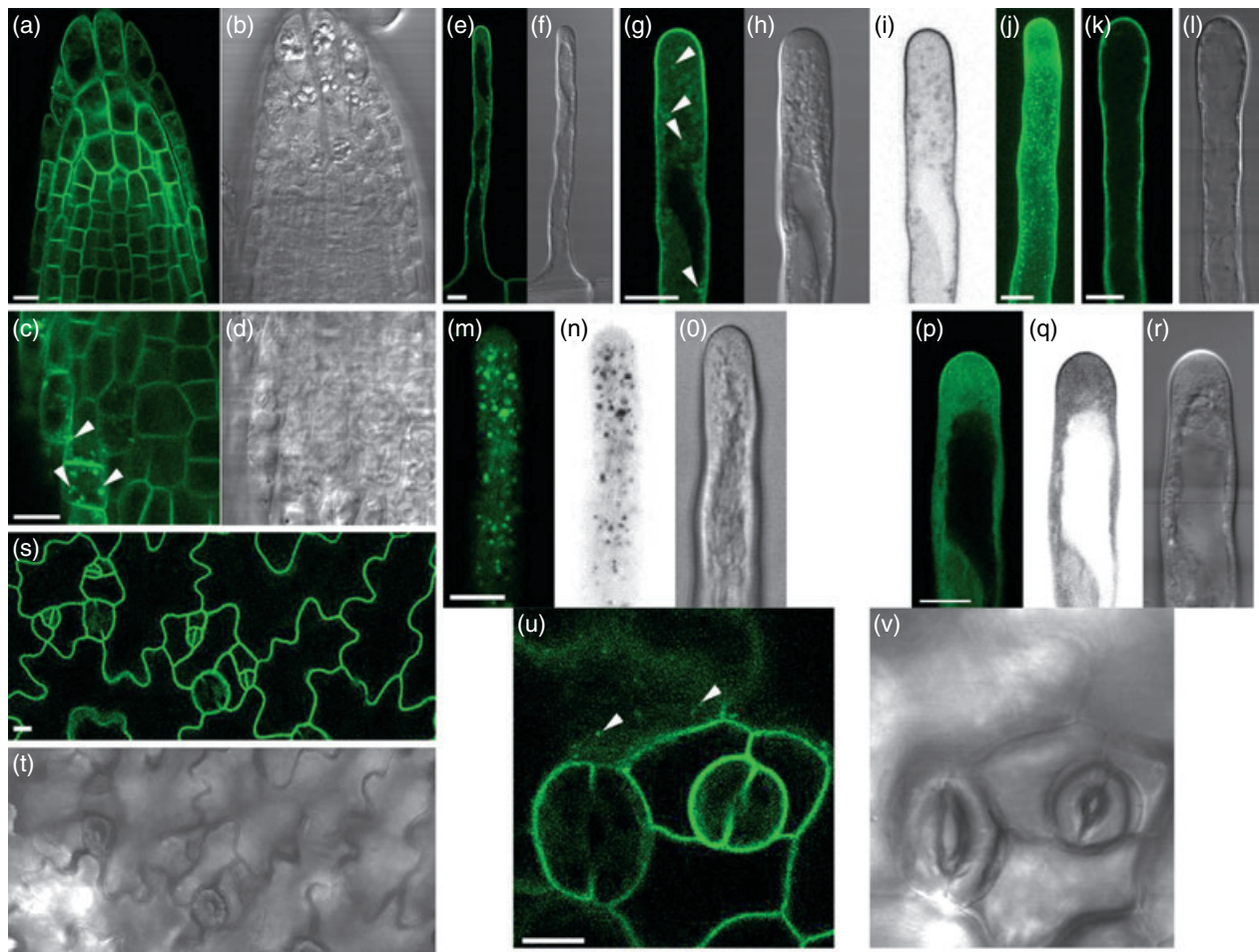


Figure 9. Localization of YFP-PH_{FAPP1} in Arabidopsis seedlings.

Confocal fluorescence images were taken for various cell types of Arabidopsis seedlings expressing YFP-PH_{FAPP1}.

(a, b) Root tip, (c, d) root cortex cells (also showing fluorescence on punctate structures), (e, f) growing root hair, (g, h) magnification of a growing root hair, (i) root hair of (g) shown in black and white to highlight the tip-localized gradient of PtdIns4P in the plasma membrane. Arrowheads indicate YFP-PH_{FAPP1}-labelled Golgi compartments. (j) Maximal projection of an image stack taken from a growing root hair, (k, l) older, non-growing root hair, (m, o) localization of YFP-2 × FYVE in a growing root hair, (n) corresponding black and white image showing no gradient, (p, r) localization of the PtdIns(4,5)P₂ biosensor YFP-PH_{PLCδ1} in a growing root hair, (q) corresponding black and white image highlighting the tip-localized gradient of YFP-PH_{PLCδ1} in the plasma membrane, (s, t) leaf epidermal cells, (u, v) guard cells. Scale bars = 50 μm (a), 10 μm (c, e, g, j, k, m, p, s, u) or 20 μm (s). (a, c, e, g, j, k, m, p, s, u) YFP fluorescence; (b, d, f, h, l, o, r, t, u) DIC images.

This tip-localized plasma membrane gradient appeared to resemble that of PtdIns(4,5)P₂, as shown previously using YFP-PH_{PLCδ1} (van Leeuwen *et al.*, 2007; Vincent *et al.*, 2005). However, as shown in Figure 9(j,q), YFP-PH_{PLCδ1} only labels the extreme tip, whereas YFP-PH_{FAPP1} labelled the whole plasma membrane, increasing in intensity towards the tip. In contrast, as indicated by YFP-2 × FYVE labelling, PtdIns3P was only present in punctate structures, probably late endosomes (Vermeer *et al.*, 2006) that were evenly distributed throughout the growing root hair (Figure 9m,n). To confirm whether the YFP-PH_{FAPP1}-labelled punctate structures were Golgi membranes, seedlings were treated with brefeldin A (BFA), a fungal toxin that inhibits Golgi trafficking, which results in the appearance of larger so-called BFA compartments (Geldner *et al.*, 2003; Ritzenthaler *et al.*, 2002).

Incubation with 50 μM BFA for 30 min resulted in the appearance of large YFP-PH_{FAPP1}-labelled compartments (Figure S8a,b). Washout of the BFA completely reversed this effect (Figure S8c,d). These results suggest that, in Arabidopsis, PtdIns4P is present on both plasma membrane and the Golgi.

Recently, it was shown that the *root hair defective 4* mutant is mutated in the AtSAC7 gene, which was shown to encode a PtdIns4P phosphatase (Thole *et al.*, 2008). *rhd4* mutants exhibited approximately 50% more PtdIns4P (Thole *et al.*, 2008). Expression of YFP-PH_{FAPP1} in *rhd4-1* revealed that most of the fluorescence was localized on internal membranes, whereas, in the wild-type background (Col-0), it was mostly the plasma membrane that was labelled (compare Figure 10a–c with Figure 10d–i), essentially confirming the results of Thole *et al.* (2008). This differential localization

Figure 10. Differential localization of YFP-PH_{FAPP1} in the PtdIns4P phosphatase mutant *rhd4-1* (*sac7-1*).

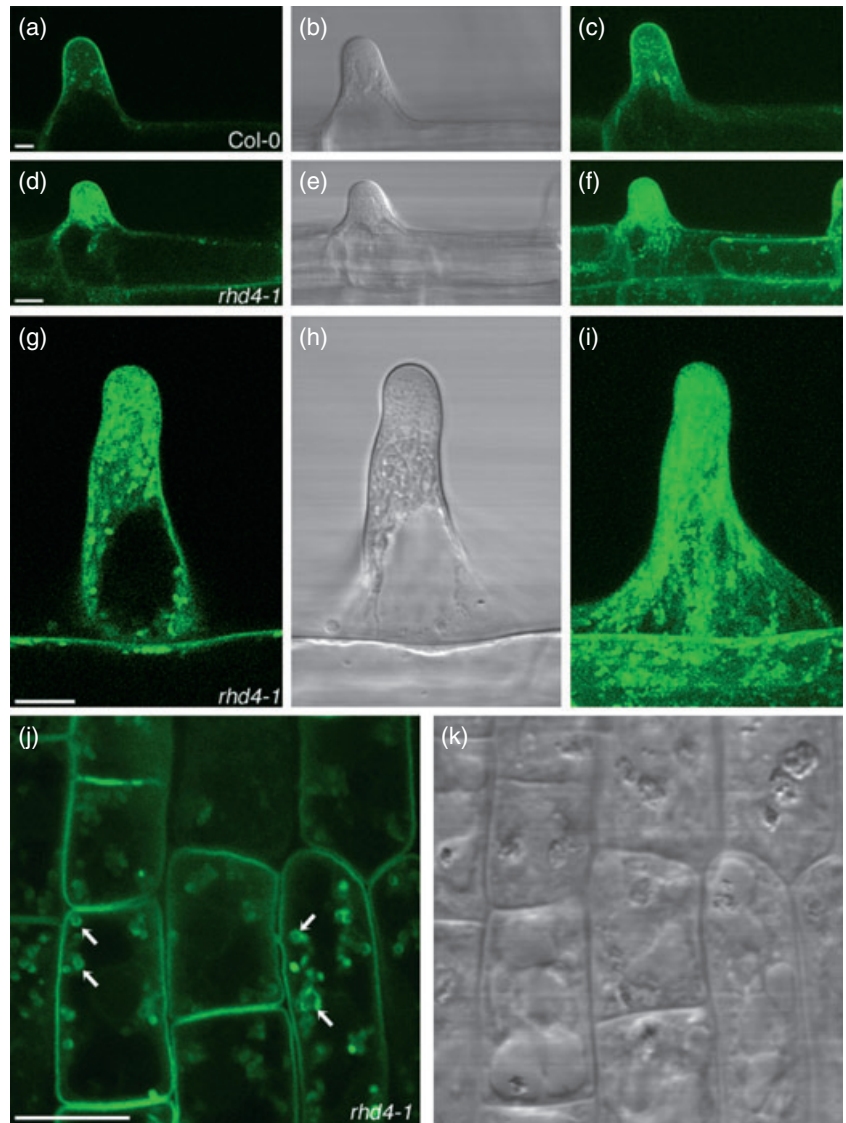
Confocal images of Col-0 (a–c) and *rhd4-1* seedlings (d–l) expressing YFP-PH_{FAPP1}.

(a, b) Emerging root hair, (c) maximal projection of an image stack taken from root hair shown in (a) showing strong labelling of the plasma membrane.

(d, e) Emerging root hair, (f) maximal projection of an image stack taken from root hair shown in (d).

(g, h) Growing root hair, (i) maximal image projection of same root hair as shown in (g). As shown in (d–i), YFP-PH_{FAPP1} accumulates on internal membranes and hardly labels the plasma membrane of mutant root hairs.

(j, k) Cells close to the root tip showing YFP-PH_{FAPP1} labelling of the plasma membrane and 'donut-like structures'. (a, c, d, f, g, i, j, l) YFP fluorescence; (b, e, h, k) DIC images. Scale bar = 10 μm.



of YFP-PH_{FAPP1} was also observed in root cells close to the tip (Figure 10j,k). In addition to strong plasma membrane labelling, accumulation of YFP-PH_{FAPP1} on enlarged Golgi structures, some of which displayed a 'donut-like' shape, was also observed (arrows in Figure 10j,k).

Discussion

Using YFP-PH_{FAPP1} as a PtdIns4P biosensor

The YFP-PH_{FAPP1} biosensor has been used to monitor PtdIns4P dynamics in animal cells (Balla *et al.*, 2005, 2008; Godi *et al.*, 2004) and yeast (Levine and Munro, 1998, 2002; Roy and Levine, 2004). Here, we describe its use to study the localization and dynamics of PtdIns4P in living plant cells. Four plant systems were tested: transient expression in cowpea protoplasts, and stable expression in tobacco BY-2

cells, *Medicago truncatula* roots and Arabidopsis seedlings. All systems allowed expression of YFP-PH_{FAPP1} without any adverse effects caused by the 35 S-driven expression of the biosensor. Point mutations in PH_{FAPP1}, known to be essential for PtdIns4P binding, revealed that the observed localization was PtdIns4P-dependent. In addition, changes in cellular PtdIns4P levels were detected (Figure 10) (Thole *et al.*, 2008). We conclude that, as in yeast mammalian cells (Balla *et al.*, 2005; Dowler *et al.*, 2000; Strahl *et al.*, 2005), YFP-PH_{FAPP1} or mRFP-PH_{FAPP1} can be used as a genuine PtdIns4P sensor in living plant cells.

Identification of multiple PtdIns4P pools in plants

Expression of YFP-PH_{FAPP1} in protoplasts labelled punctate structures moving through the cytosol and the plasma membrane (Figure 1). Similar labelling patterns were

observed in stably transformed BY-2 cells, *M. truncatula* roots and *Arabidopsis* seedlings (Figures 2, 8 and 9). This suggests that plants contain two spatially separated PtdIns4P pools. An additional lower level of fluorescence in the cytoplasm and nucleoplasm probably reflects the dynamic equilibrium between binding and non-binding that is typical for these biosensors (Balla, 2007; van Leeuwen *et al.*, 2007; Vermeer, 2006).

Using co-expression studies with various markers, YFP-PH_{FAPP1} clearly co-localized with the Golgi marker STtmd-CFP but not with the endocytic/pre-vacuolar marker GFP-AtRABF2b. BY-2 cells co-expressing mRFP-PH_{FAPP1} and YFP-2 × FYVE, which binds PtdIns3P and labels a late endocytic compartment (Vermeer *et al.*, 2006), also showed no overlap in fluorescence, emphasizing that the PtdIns3P- and PtdIns4P pools are spatially separated. When observed in more detail, the punctate mRFP-PH_{FAPP1} structures were frequently found in close proximity to the YFP-2 × FYVE-labelled compartments, resembling the observations in BY-2 cells stably expressing YFP-2 × FYVE and STtmd-CFP (Vermeer *et al.*, 2006). Together these data suggest that plant cells contain at least two distinct PtdIns4P pools: plasma membrane and the Golgi.

PtdIns4P localization may be functionally conserved because yeast and mammalian cells also revealed these two pools (Audhya and Emr, 2002; Balla *et al.*, 2005; Roy and Levine, 2004; Weixel *et al.*, 2005). However, while in yeast and mammalian cells, YFP-PH_{FAPP1} is mainly localized to the Golgi (Balla *et al.*, 2005; Levine and Munro, 2001, 2002), it is clearly the plasma membrane that is predominantly labelled in plant cells. In mammalian cells, the plasma membrane is only clearly labelled after receptor stimulation (Balla *et al.*, 2005; Levine and Munro, 2001, 2002).

PtdIns4P synthesis is catalysed by PI 4-kinases. These enzymes are classified as type II or III forms (type I was found to be a PI 3-kinase) based on their enzymatic properties and size (Balla, 1998; Balla and Balla, 2006). Type III kinases are relatively large, usually soluble and sensitive to wortmannin, whereas the smaller type II enzymes are particulate and insensitive to this inhibitor.

The yeast *Saccharomyces cerevisiae* contains three PI 4-kinases, encoded by Pik1p, Stt4p (both type III) and Lsb6p (type II). Knockout strains of *Lsb6p* exhibit no significant differences in PtdIns4P levels and are viable, whereas the *Pik1p* and *Stt4p* genes are essential and are responsible for at least 95% of the PtdIns4P pool (Audhya and Emr, 2002; Han *et al.*, 2002; Shelton *et al.*, 2003). Pik1p genetically interacts with Sec14p and is important for exocytic trafficking from the Golgi (Hama *et al.*, 1999; Walch-Solimena and Novick, 1999). The PtdIns4P generated by Pik1p facilitates the binding of Kes1p to the Golgi, a factor that controls the function of the small G-protein ARF (ADP-ribosylation factor) and budding (Li *et al.*, 2002). A temperature-sensitive mutant of Pik1p exhibits defects in endocytosis and vacuolar

dynamics (Audhya *et al.*, 2000). Pik1p has also been suggested to play an essential role in the nucleus but this could be independent of its kinase activity, as no nuclear labelling by GFP-PH_{FAPP1} was observed (Strahl *et al.*, 2005). In contrast, Stt4p binds to the plasma membrane via the protein Sfk1p, where it promotes cell-wall assembly and cytoskeletal rearrangements (Audhya and Emr, 2002; Audhya *et al.*, 2000). Lsb6p plays a role in actin-dependent endosome motility; however, this is independent of its PI 4-kinase activity (Chang *et al.*, 2005).

In mammalian cells, four PI 4-kinases have been identified, i.e. α and β isoforms for both type II and III enzymes (Balla *et al.*, 2002, 2005, 2008; Godi *et al.*, 1999; Weixel *et al.*, 2005). Type II enzymes are present in various cellular membranes but enriched in the plasma membrane and have been suggested to play a role in post-trans-Golgi network trafficking. Nonetheless, the plasma membrane localization of PtdIns4P was recently shown to be dependent on the activity of wortmannin-sensitive, type III PI4 kinases, particularly PI4KIII α (Balla *et al.*, 2008).

In *Arabidopsis*, 12 PI 4-kinase genes have been predicted, which have been classified into three subfamilies: α 1–2 and β 1–2 (all type III) and γ 1–8 (type II). So far, lipid kinase activity has only been shown for AtPI4K α 1 and AtPI4K β 1 (Stevenson-Paulik *et al.*, 2003). Moreover, it is possible that the γ subfamily represents protein kinases rather than lipid kinases (Galvão *et al.*, 2008). GFP localization experiments for AtPI4K α 1 and β 1 in insect cells revealed that the proteins were confined to distinct punctate structures and absent from the plasma membrane (Stevenson-Paulik *et al.*, 2003). Immunolocalization studies on AtPI4K β 1 in growing root hairs of *Arabidopsis* revealed co-localization with a Rab GTPase on Golgi membranes, concentrated at the tip (Preuss *et al.*, 2006). It will be interesting to determine which kinase(s) is/are responsible for the relatively large plasma membrane pool of PtdIns4P.

Do PAO and wortmannin inhibit PI 4-kinase activity in plant cells?

Wortmannin is a typical PI 3-kinase inhibitor, but at higher concentrations is also able to inhibit mammalian type III PI 4-kinase activity, presumably because the kinase domains closely resemble each other. PAO also inhibits type III PI 4-kinase activity and is relatively ineffective against type II enzymes. The mechanism by which this sulfhydryl-reactive agent works is unknown (Balla *et al.*, 2008). In plant extracts, a relatively high concentration of wortmannin (30 μ M) has been reported to inhibit PI 4-kinase activity *in vitro* (Matsuoka *et al.*, 1995). *In vivo* analysis, using ³²P-labelled BY-2 cells and HPLC headgroup analysis of PPIs revealed that wortmannin reduced the PtdIns3P levels by more than one-third within 15 min of treatment and that the ³²P-labelling of PtdIns4P was also slightly affected, being reduced by

approximately 5–10% (Vermeer *et al.*, 2006). Wortmannin had no effect on the localization of mRFP-PH_{FAPP1}, even with the higher 30 μM concentration, while that of YFP-2 \times FYVE was dramatically affected (Figure 6i–p and Figure S4). In contrast, treatment of cells with 20 μM PAO resulted in a rapid loss of membrane labelling by mRFP-PH_{FAPP1} in both plasma membrane and punctate structures (Fig 6a–d), while YFP-2 \times FYVE labelling was hardly affected. We also observed a strong effect on cytoplasmic streaming and vacuolar morphology of the cells. However, ³²P radiolabelling experiments did not reveal any changes in ³²P-PtdInsP levels (Figure S3). However, using longer labelling times, we did observe that PAO treatment resulted in a decrease of ³²P-labelled structural lipids (data not shown). This could mean that PAO is toxic to the cells, rather than acting as a PI 4-kinase-specific inhibitor. However, this does not explain why the mRFP-PH_{FAPP1} localization was affected whereas localization of YFP-2 \times FYVE was not. It should be noted that in another system, Arabidopsis suspension cells, Krinke *et al.* (2007) reported that PAO could inhibit PI 4-kinase activation.

Together, these results indicate that, in tobacco BY-2 cells, wortmannin primarily acts an inhibitor for PI 3-kinase and not PI 4-kinase activity. As PtdIns3P is involved in various membrane trafficking events, it is not unlikely that wortmannin has a small indirect effect on PtdIns4P synthesis. Our data also show that the results obtained with PAO should be interpreted with caution.

Role for PtdIns4P during plant cytokinesis

Recently, Dhonukshe *et al.* (2006) showed that cell-plate initiation can still occur in the absence of Golgi stacks and/or protein synthesis. Moreover, they provided evidence that endocytic material was required to form this cell plate (Dhonukshe *et al.*, 2006). In dividing BY-2 cells co-expressing mRFP-PH_{FAPP1} and YFP-2 \times FYVE, we show that PtdIns3P is completely excluded from the cell plate, whereas PtdIns4P is strongly enriched. Previously, we found that PtdIns3P-containing compartments completely surround the expanding cell plate (Vermeer *et al.*, 2006) and that wortmannin was able to delay cell-plate formation (Dhonukshe *et al.*, 2006). These data imply that, although PtdIns3P does not localize to the cell plate, it could have a role in the transport of membrane vesicles to or from the growing cell plate. The fact that we found PtdIns4P on Golgi stacks and on the forming cell plate could mean that there is a flow of vesicles from the Golgi to the cell plate. However, no Golgi stacks were found in close proximity to the cell plate during its initiation, and when BFA was used, Golgi compartments were dissolved, but this did not abolish cell-plate initiation (Dhonukshe *et al.*, 2006). This suggests that the PtdIns4P in the cell plate is not derived from vesicle flow from the Golgi. Using co-labelling with the endocytic tracer FM4-64, we found that FM4-64 labelled the cell plate slightly

earlier than did YFP-PH_{FAPP1} (Figure 7c,d and Movie S10). This implies that PtdIns4P is synthesized locally by a cell plate-associated PI 4-kinase, although we cannot exclude the possibility that some PtdIns4P also enters the cell plate via active transport (Golgi or endocytosis). Knockout mutants of PI 4-kinases and GFP-tagged versions of the enzymes may shed further light on this in the near future. The fact that Arabidopsis *pi4k β 1 β 2* double mutants only exhibit a slight cytokinetic phenotype (E.N., unpublished results) indicates a role for PtdIns4P in cell-plate expansion rather than initiation.

Does PtdIns4P regulate tip growth?

Previously, a PtdIns(4,5) P_2 gradient in the plasma membrane of growing root hairs and pollen tubes has been implicated in regulating tip growth (Dowd *et al.*, 2006; Helling *et al.*, 2006; Kost *et al.*, 1999; van Leeuwen *et al.*, 2007; Vincent *et al.*, 2005). This gradient was proposed to be created by local stimulation of PtdIns4P 5-kinase activity via a Rop GTPase (Kost *et al.*, 1999). Our observation here, that PtdIns4P is already present in a tip-localized gradient, implies that it is not necessarily the regulation of the PtdIns4P 5-kinase that creates the PtdIns(4,5) P_2 gradient, as a uniformly spatial distributed kinase would also create this. Recently, an Arabidopsis PI 4-kinase that plays a crucial role in the polarized expansion of root hairs has been identified (Preuss *et al.*, 2006). This AtPI4K β 1 localizes to the tip of growing root hairs through interaction with a Rab GTPase and a Ca²⁺ sensor. Together, this was proposed to result in tip-localized PI 4-kinase activity, with subsequent enrichment of PtdIns4P (Preuss *et al.*, 2006). Our data confirm this hypothesis. More recently, a root hair mutant exhibiting huge defects in polarity (bulging, swelling) was discovered to carry a mutation in a PtdIns4P phosphatase (Thole *et al.*, 2008). Together, these data indicate an essential role for PtdIns4P in polar tip growth. Recent data on a PtdIns4P 5-kinase mutant (AtPIP5K3) exhibiting a root hair phenotype indicate that PtdIns(4,5) P_2 is more important for growth rather than polarity (Kusano *et al.*, 2008; Stenzel *et al.*, 2008). The observation of enlarged Golgi structures in *rhd4-1* suggests that proper regulation of PtdIns4P levels at the Golgi is required for maintaining its structure.

It is still not known what the precise function of PtdIns4P is. In general, PtdIns4P is usually regarded as the precursor of PtdIns(4,5) P_2 , which has emerged as a very important signalling molecule in three ways: (i) as a substrate for PI 3-kinase signalling to produce the lipid second messenger PtdIns(3,4,5) P_3 ; (ii) as substrate for PLC signalling, generating the second messengers Ins P_3 , which release calcium from intracellular stores, and diacylglycerol (DAG), which activates protein kinase C (PKC); and (iii) as a second messenger itself, targeting proteins to membranes via specific lipid-binding domains, regulating ion-channel

activity, organizing the actin cytoskeleton and modulating vesicular trafficking (for review, see Gamper and Shapiro, 2007; Huang, 2007; McLaughlin *et al.*, 2002). While these signalling systems have been clearly established in mammalian cells over the last decade (van Leeuwen *et al.*, 2007), a completely different picture is emerging for plants. There is no PI 3-kinase that phosphorylates PtdIns(4,5) P_2 into PtdIns(3,4,5) P_3 , there is no Ca^{2+} -gated Ins P_3 receptor, and no PKC homologues have been identified in plants (Zonia and Munnik, 2006). In the past, Ins P_3 has been shown to release Ca^{2+} from intracellular stores when micro-injected or released via photo-activation of a caged variant, but work from Brearley's lab shows this is probably caused by Ins P_6 (Lemtiri-Chlieh *et al.*, 2003; Zonia and Munnik, 2006). The latter can release Ca^{2+} at a 10-fold lower concentration than Ins P_3 , and, when Ins P_3 is micro-injected, it is rapidly converted into Ins P_6 . The hormonal stimulation via ABA to which it was linked was also shown to generate an Ins P_6 response rather than Ins P_3 (Lemtiri-Chlieh *et al.*, 2003). In yeast, Ins P_6 signalling is not related to Ca^{2+} but directly regulates gene transcription and mRNA export from the nucleus. The pathway involves PLC and two inositol polyphosphate multi-kinases that can stepwise phosphorylate Ins P_3 to Ins P_6 (Ives *et al.*, 2000; Odom *et al.*, 2000; Perera *et al.*, 2004; York *et al.*, 1999, 2001).

Another difference is that the PtdIns(4,5) P_2 concentrations in higher plants are extremely low compared to those of mammalian cells or green algae. The latter systems usually have a 1:1 ratio of PtdIns4 P and PtdIns(4,5) P_2 , whereas higher plant cells exhibit 30–100-fold lower PtdIns(4,5) P_2 ratios (van Leeuwen *et al.*, 2007; Munnik *et al.*, 1994a). The huge difference in PtdIns4 P and PtdIns(4,5) P_2 levels shows that PtdIns4 P cannot be simply regarded as a precursor of PtdIns(4,5) P_2 . Their differential localization during, for example, cell-plate formation (this study; van Leeuwen *et al.*, 2007)) also suggests this, as do the strong mutant phenotypes with respect to root hair growth of a PI 4-kinase (Preuss *et al.*, 2006) and PtdIns4 P 4-phosphatase (Thole *et al.*, 2008), as opposed to the weak phenotype of a phosphatidylinositol 4-phosphate 5-kinase mutant (Kusano *et al.*, 2008; Stenzel *et al.*, 2008).

We anticipate that PtdIns4 P fulfils additional signalling roles. Arabidopsis is predicted to contain more than 50 proteins with a pleckstrin homology domain (van Leeuwen *et al.*, 2004). For most of them, it is still unknown which phosphoinositide they bind or whether they bind at all, but, as for the human FAPP1 protein, PtdIns4 P might be a targeting determinant itself. Alternatively, PtdIns4 P might be responsible for many of the effects shown for mammalian PtdIns(4,5) P_2 , e.g. regulating the actin cytoskeleton or ion-channel activity (Hilgemann *et al.*, 2001; Hilpela *et al.*, 2004). PtdIns4 P could also be the substrate for PLC, generating Ins(1,4) P_2 that is phosphorylated to Ins P_6 (Zonia and Munnik, 2006). Alternatively, PLC could simply function as a PtdIns4 P

attenuator. *In vitro*, plant phosphoinositide specific phospholipase C (PI-PLCs) do not distinguish between PtdIns4 P or PtdIns(4,5) P_2 (reviewed by Munnik *et al.*, 1998). So far, we have assumed that PtdIns(4,5) P_2 is the *in vivo* substrate only because of the mammalian paradigm.

Whatever the function of PtdIns4 P turns out to be, the use of lipid biosensors together with mutant analyses will be of great help in further uncovering its role in cell signalling and membrane trafficking.

Experimental procedures

Constructs

All constructs were produced using standard molecular biological methods. To create pEYFP-PH_{FAPP1} and pmRFP-PH_{FAPP1}, the pleckstrin homology domain of HsFAPP1 were amplified from plasmid pEGFP-PH_{FAPP1}, kindly provided by Dr T. Levine (Institute of Ophthalmology, London, UK) using primers FAPP1Bgl2fw (5'-GAAGA-TCTATGGAGGGGGTGTGTAC-3') and FAPP1TEcorev (5'-CGGAA-TTCTATGTATCAGTCAAACATGC-3' [restriction sites are underlined]). Subsequently, the pleckstrin homology domain was cloned behind EYFP or mRFP using *Bgl*II and *Eco*RI. The EYFP/mRFP-PH_{FAPP1} fusions were excised using *Nhe*I and *Eco*RI, and transferred to pMONd35 S using its *Xba*I and *Eco*RI sites. The plasmid containing mRFP1 was kindly provided by Dr R.Y. Tsien (University of California, La Jolla, CA, USA). To generate the point mutations in the pleckstrin homology domains of HsFAPP1, the primers FAPP1-K7Efw (5'-CTATGGAGGGGGTGTGTACGAGTGGACCACTATCTCACAGGC-3') and FAPP1K7Erev (5'-GCCTGTGAGATAGTTGGTCCACTCGTACAACACCCCTCCATAG-3') were used. To generate pMONd35S::YFP-PH_{FAPP1-R18L}, the PH_{FAPP1} domain was amplified from plasmid pEGFP-diFAPP1R18L (kindly provided by Dr M.A. de Matteis, Consorzio Mario Negri Sud, Santa Maria Imbaro, Italy) using the same primers and strategy as described for pMONd35S::YFP-PH_{FAPP1}. To generate stably transformed *A. thaliana* plants, both YFP-PH_{FAPP1} and mRFP-PH_{FAPP1-K7E} were transferred to pCAMBIA-35 S using *Nco*I/*Eco*RI and *Nhe*I/*Eco*RI, respectively. The plasmid bearing GFP-ARA7 was kindly provided by Dr A. Nakano (RIKEN, Tokyo, Japan). For BY-2 cell and *Medicago truncatula* root transformation, all fusions were cloned into the pCambia35S vector. pBINJV-35 S::YFP-2 × FYVE and pBIN35S::STtmd-CFP have been described previously (Vermeer *et al.*, 2006).

Transient expression in cowpea protoplasts

Cowpea (*Vigna unguiculata* L.) protoplasts were prepared from 10-day-old plants and transfected with 10 µg of plasmid DNA using the polyethylene glycol method as described previously (Vermeer *et al.*, 2004).

³²P_i phospholipid labelling, extraction and analysis

BY-2 cells (5–6 days old, sub-cultured weekly) were pre-labelled with ³²PO₄³⁻ (carrier-free, PerkinElmer, <http://www.perkinelmer.nl>) for 5 min and subsequently treated with an equal volume of cell-free medium containing 40 µM PAO or 0.1% DMSO as a control for the solvent. Lipids were extracted, separated by TLC and quantified by phosphoimaging as described previously (Vermeer *et al.*, 2006).

Stable transformations

Tobacco BY-2 cells were transformed and sub-cultured as described previously (Vermeer *et al.*, 2006). For stable expression of GFP fusions in *Medicago truncatula* (Jemalong A17), *Agrobacterium rhizogenes*-mediated root transformation was performed as described by Limpens *et al.* (2004). Transgenic roots were selected for fluorescence using a Leica MZFLIII stereo fluorescence microscope (<http://www.leica-microsystems.com>). Fluorescent roots were mounted between two cover glasses in liquid root medium [Gamborg B5 medium including vitamins (Duchefa, <http://www.duchefa.nl>) supplemented with 3% sucrose, pH 5.8]. *Arabidopsis thaliana* cv. Columbia plants were transformed using floral-dip transformation (Clough and Bent, 1998). Homozygous T₃ plants were used for further analysis. Seeds were germinated on 0.5 × MS containing 1% sucrose and 0.9% agar.

Confocal microscopy

BY-2 cells (4–5 days old) or protoplasts (17 h after transfection) were mounted in eight-chambered cover slides (Nalge Nunc International, <http://www.nuncbrand.com>). *Arabidopsis* seedlings were imaged as described previously (Vermeer *et al.*, 2006). Fluorescence microscopy was performed using a Zeiss LSM 510 confocal laser scanning microscope (<http://www.zeiss.com/>), implemented on an inverted microscope (Zeiss Axiovert 100). Excitation was provided by the 458, 488 and 514 nm Ar laser, 543 nm HeNe and 568 nm Kr lines, controlled by an acousto-optical tuneable filter. For YFP/chlorophyll fluorescence, we used excitation/emission combinations of 514 nm/band pass 530–600 for YFP and long pass 650 for chlorophyll in combination with the HFT458/514 primary, NFT635 secondary and NFT515 tertiary dichroic splitters. For YFP/FM4-64 fluorescence, we used excitation/emission combinations of 488 nm/band pass 505–550 for YFP and 543 nm/long pass P650 for FM4-64 in combination with HFT 488/543 primary and NFT545 secondary dichroic splitters. For CFP/YFP/chlorophyll detection, we used the excitation/emission combinations of 458 nm/band pass 470–500 for CFP and 514 nm/band pass 530–600 for YFP in combination with the HFT458/514 primary, NFT635 secondary and NFT490 tertiary dichroic splitters. For GFP/YFP/chlorophyll detection, settings were used as described for CFP/YFP/chlorophyll detection.

For YFP/mRFP dual scanning, we used the excitation/emission combinations of 488 nm/band pass 505–550 for YFP and 568 nm/long pass 585 for mRFP in combination with the HFT488/568 primary, NFT570 secondary and NFT515 tertiary dichroic splitters. Cross-talk-free images were acquired by operating the microscope in the multi-tracking mode. A Zeiss water-immersion C-Apochromat 40 × objective lens (numerical aperture 1.2), corrected for cover glass thickness, was used for scanning. Images were captured and analyzed using ZEISS LSM510 software (version 3.2 SP3).

Acknowledgements

We thank Tim Levine (Institute of Ophthalmology, London, UK), Maria Antonietta De Matteis (Consorzio Mario Negri Sud, Santa Maria Imbaro, Italy), Akihiko Nakano (RIKEN, Tokyo, Japan), and Roger Tsien (University of California, La Jolla, CA, USA) for kindly providing us with various constructs. This work was supported by the Netherlands Organization for Scientific Research (NWO), Earth and Life Sciences (ALW) project numbers 810.66.012 and 864.05.001. T.W.J.G.'s lab was additionally supported by the EU integrated project on Molecular Imaging (LSHG-CT-2003-503259) and T.M.'s lab by NWO grant numbers 810.66.011, 813.06.003,

864.05.001 and 700.56.007 and the Royal Netherlands Academy of Arts and Sciences (KNAW).

Supporting Information

Additional Supporting Information may be found in the online version of this article:

Figure S1. Localization of various YFP-PH_{FAPP1} constructs in mammalian cells.

Figure S2. Stable expression of mRFP-PH_{FAPP1} in tobacco BY-2 cells.

Figure S3. Effect of 20 μM PAO on ³²P-PtdInsP levels in tobacco BY-2 cells.

Figure S4. Effect of 30 μM wortmannin on the localization of mRFP-PH_{FAPP1} and YFP-2 × FYVE.

Figure S5. Localization of PH_{FAPP1} fusion is PtdIns4P-dependent.

Figure S6. YFP-PH_{FAPP1} is present as a tip-localized plasma membrane gradient in growing *Arabidopsis* root hairs.

Figure S7. YFP-PH_{FAPP1} is not present as a tip-localized plasma membrane gradient in a root hair that has stopped growing.

Figure S8. Effect of 50 μM BFA on the localization of YFP-PH_{FAPP1} in *A. thaliana*.

Movie S1. mRFP-PH_{FAPP1} is present on the plasma membrane and motile punctate structures.

Movie S2. Absence of co-labelling of YFP-PH_{FAPP1} and FM4-64.

Movie S3. mRFP-PH_{FAPP1} labels PtdIns4P at the Golgi membranes.

Movie S4. Co-expression of mRFP-PH_{FAPP1} and YFP-2 × FYVE in stably transformed BY-2 cells.

Movie S5. Effect of the PI 4-kinase inhibitor phenylarsine oxide (PAO) on mRFP-PH_{FAPP1} and YFP-2 × FYVE labelling over 20 min.

Movie S6. Effect of the PI 4-kinase inhibitor phenylarsine oxide (PAO) on mRFP-PH_{FAPP1} and YFP-2 × FYVE labelling over 45 min.

Movie S7. Effect of the PI 3-kinase inhibitor wortmannin (WM) on mRFP-PH_{FAPP1} and YFP-2 × FYVE labelling over 20 min.

Movie S8. Effect of the PI 3-kinase inhibitor wortmannin (WM) on mRFP-PH_{FAPP1} and YFP-2 × FYVE labelling over 45 min.

Movie S9. Dynamics of PtdIns3P and PtdIns4P during cell division in BY-2 cells.

Movie S10. Dynamics of PtdIns4P and FM4-64-labelled membranes during cell division in BY-2 cells.

Please note: Wiley-Blackwell are not responsible for the content or functionality of any supporting materials supplied by the authors. Any queries (other than missing material) should be directed to the corresponding author for the article.

References

- Arcaro, A. and Wymann, M.P. (1993) Wortmannin is a potent phosphatidylinositol 3-kinase inhibitor: the role of phosphatidylinositol 3,4,5-trisphosphate in neutrophil responses. *Biochem. J.* **296**, 297–301.
- Audhya, A. and Emr, S.D. (2002) Stt4 PI 4-kinase localizes to the plasma membrane and functions in the Pkc1-mediated MAP kinase cascade. *Dev. Cell.* **2**, 593–605.
- Audhya, A., Foti, M. and Emr, S.D. (2000) Distinct roles for the yeast phosphatidylinositol 4-kinases, Stt4p and Pik1p, in secretion, cell growth, and organelle membrane dynamics. *Mol. Biol. Cell.* **11**, 2673–2689.
- Balla, T. (1998) Phosphatidylinositol 4-kinases. *Biochim. Biophys. Acta.* **1436**, 69–85.
- Balla, T. (2007) Imaging and manipulating phosphoinositides in living cells. *J. Physiol.* **582**, 927–937.
- Balla, A. and Balla, T. (2006) Phosphatidylinositol 4-kinases: old enzymes with emerging functions. *Trends Cell Biol.* **16**, 351–361.

- Balla, A., Tuymetova, G., Barshishat, M., Geiszt, M. and Balla, T.** (2002) Characterization of type II phosphatidylinositol 4-kinase isoforms reveals association of the enzymes with endosomal vesicular compartments. *J. Biol. Chem.* **277**, 20041–20050.
- Balla, A., Tuymetova, G., Tsiomenko, A., Varnai, P. and Balla, T.** (2005) A plasma membrane pool of phosphatidylinositol 4-phosphate is generated by phosphatidylinositol 4-kinase type-III α : studies with the PH domains of the oxysterol binding protein and FAPP1. *Mol. Biol. Cell.* **16**, 1282–1295.
- Balla, A., Kim, Y.J., Varnai, P., Szentpetery, Z., Knight, Z., Shokat, K.M. and Balla, T.** (2008) Maintenance of hormone-sensitive phosphoinositide pools in the plasma membrane requires phosphatidylinositol 4-kinase III α . *Mol. Biol. Cell.* **19**, 711–721.
- Boevink, P., Oparka, K., Santa Cruz, S., Martin, B., Betteridge, A. and Hawes, C.** (1998) Stacks on tracks: the plant Golgi apparatus traffics on an actin/ER network. *Plant J.* **15**, 441–447.
- Boisson-Dernier, A., Chabaud, M., Garcia, F., Becard, G., Rosenberg, C. and Barker, D.G.** (2001) *Agrobacterium rhizogenes*-transformed roots of *Medicago truncatula* for the study of nitrogen-fixing and endomycorrhizal symbiotic associations. *Mol. Plant-Microbe Interact.* **14**, 695–700.
- Bolte, S., Talbot, C., Boutte, Y., Catrice, O., Read, N.D. and Satiat-Jeuemaitre, B.** (2004) FM-dyes as experimental probes for dissecting vesicle trafficking in living plant cells. *J. Microsc.* **214**, 159–173.
- Chang, F.S., Han, G.S., Carman, G.M. and Blumer, K.J.** (2005) A WASp-binding type II phosphatidylinositol 4-kinase required for actin polymerization-driven endosome motility. *J. Cell Biol.* **171**, 133–142.
- Clough, S.J. and Bent, A.F.** (1998) Floral dip: a simplified method for *Agrobacterium*-mediated transformation of *Arabidopsis thaliana*. *Plant J.* **16**, 735–743.
- Corvera, S., D'Arrigo, A. and Stenmark, H.** (1999) Phosphoinositides in membrane traffic. *Curr. Opin. Cell Biol.* **11**, 460–465.
- Dhonukshe, P., Baluska, F., Schlicht, M., Hlavacka, A., Samaj, J., Friml, J. and Gadella, T.W. Jr** (2006) Endocytosis of cell surface material mediates cell plate formation during plant cytokinesis. *Dev. Cell.* **10**, 137–150.
- Dowd, P.E., Coursol, S., Skirpan, A.L., Kao, T.H. and Gilroy, S.** (2006) *Petunia* phospholipase c1 is involved in pollen tube growth. *Plant Cell*, **18**, 1438–1453.
- Dowler, S., Currie, R.A., Campbell, D.G., Deak, M., Kular, G., Downes, C.P. and Alessi, D.R.** (2000) Identification of pleckstrin-homology-domain-containing proteins with novel phosphoinositide-binding specificities. *Biochem. J.* **351**, 19–31.
- Galvão, R.M., Kota, U., Soderblom, E.J., Goshe, M.B. and Boss, W.F.** (2008) Characterization of a new family of protein kinases from *Arabidopsis* containing phosphoinositide 3/4-kinase and ubiquitin-like domains. *Biochem. J.* **409**, 117–127.
- Gamper, N. and Shapiro, M.S.** (2007) Regulation of ion transport proteins by membrane phosphoinositides. *Nature Rev.* **8**, 921–934.
- Geldner, N., Anders, N., Wolters, H., Keicher, J., Kornberger, W., Muller, P., Delbarre, A., Ueda, T., Nakano, A. and Jurgens, G.** (2003) The *Arabidopsis* GNOM ARF-GEF mediates endosomal recycling, auxin transport, and auxin-dependent plant growth. *Cell*, **112**, 219–230.
- Godi, A., Pertile, P., Meyers, R., Marra, P., Di Tullio, G., Iurisci, C., Luini, A., Corda, D. and De Matteis, M.A.** (1999) ARF mediates recruitment of PtdIns-4-OH kinase-beta and stimulates synthesis of PtdIns(4,5)P₂ on the Golgi complex. *Nature Cell Biol.* **1**, 280–287.
- Godi, A., Di Campli, A., Konstantakopoulos, A., Di Tullio, G., Alessi, D.R., Kular, G.S., Daniele, T., Marra, P., Lucocq, J.M. and De Matteis, M.A.** (2004) FAPPs control Golgi-to-cell-surface membrane traffic by binding to ARF and PtdIns(4)P. *Nature Cell Biol.* **6**, 393–404.
- Gozani, O., Karuman, P., Jones, D.R. et al.** (2003) The PHD finger of the chromatin-associated protein ING2 functions as a nuclear phosphoinositide receptor. *Cell*, **114**, 99–111.
- Hama, H., Schnieders, E.A., Thorner, J., Takemoto, J.Y. and DeWald, D.B.** (1999) Direct involvement of phosphatidylinositol 4-phosphate in secretion in the yeast *Saccharomyces cerevisiae*. *J. Biol. Chem.* **274**, 34294–34300.
- Han, G.S., Audhya, A., Markley, D.J., Emr, S.D. and Carman, G.M.** (2002) The *Saccharomyces cerevisiae* LSB6 gene encodes phosphatidylinositol 4-kinase activity. *J. Biol. Chem.* **277**, 47709–47718.
- Helling, D., Possart, A., Cottier, S., Klahre, U. and Kost, B.** (2006) Pollen tube tip growth depends on plasma membrane polarization mediated by tobacco PLC3 activity and endocytic membrane recycling. *Plant Cell*, **18**, 3519–3534.
- Hilgemann, D.W., Feng, S. and Nasuhoglu, C.** (2001) The complex and intriguing lives of PIP2 with ion channels and transporters. *Sci. STKE.* **2001**, RE19.
- Hilpela, P., Vartiainen, M.K. and Lappalainen, P.** (2004) Regulation of the actin cytoskeleton by PI(4,5)P₂ and PI(3,4,5)P₃. *Curr. Topics Microbiol. Immunol.* **282**, 117–163.
- Huang, C.L.** (2007) Complex roles of PIP2 in the regulation of ion channels and transporters. *Am. J. Physiol.* **293**, F1761–F1765.
- Ives, E.B., Nichols, J., Wentte, S.R. and York, J.D.** (2000) Biochemical and functional characterization of inositol 1,3,4,5,6-pentakisphosphate 2-kinases. *J. Biol. Chem.* **275**, 36575–36583.
- Kim, D.H., Eu, Y.J., Yoo, C.M., Kim, Y.W., Pih, K.T., Jin, J.B., Kim, S.J., Stenmark, H. and Hwang, I.** (2001) Trafficking of phosphatidylinositol 3-phosphate from the trans-Golgi network to the lumen of the central vacuole in plant cells. *Plant Cell*, **13**, 287–301.
- Kost, B., Lemichez, E., Spielhofer, P., Hong, Y., Tolias, K., Carpenter, C. and Chua, N.H.** (1999) Rac homologues and compartmentalized phosphatidylinositol 4,5-bisphosphate act in a common pathway to regulate polar pollen tube growth. *J. Cell Biol.* **145**, 317–330.
- Krinke, O., Ruelland, E., Valentova, O., Vergnolle, C., Renou, J.P., Tacconat, L., Flemr, M., Burketova, L. and Zachowski, A.** (2007) Phosphatidylinositol 4-kinase activation is an early response to salicylic acid in *Arabidopsis* suspension cells. *Plant Physiol.* **144**, 1347–1359.
- Kusano, H., Testerink, C., Vermeer, J.E., Tsuge, T., Shimada, H., Oka, A., Munnik, T. and Aoyama, T.** (2008) The *Arabidopsis* phosphatidylinositol phosphate 5-kinase PIP5K3 is a key regulator of root hair tip growth. *Plant Cell*, **20**, 367–380.
- Lee, G.J., Sohn, E.J., Lee, M.H. and Hwang, I.** (2004) The *Arabidopsis* rab5 homologs rha1 and ara7 localize to the prevacuolar compartment. *Plant Cell Physiol.* **45**, 1211–1220.
- van Leeuwen, W., Ókrész, L., Bögre, L. and Munnik, T.** (2004) Learning the lipid language of plant signalling. *Trends Plant Sci.* **9**, 378–384.
- van Leeuwen, W., Vermeer, J.E., Gadella, T.W. Jr and Munnik, T.** (2007) Visualization of phosphatidylinositol 4,5-bisphosphate in the plasma membrane of suspension-cultured tobacco BY-2 cells and whole *Arabidopsis* seedlings. *Plant J.* **52**, 1014–1026.
- Lemtiri-Chlieh, F., MacRobbie, E.A., Webb, A.A., Manison, N.F., Brownlee, C., Skepper, J.N., Chen, J., Prestwich, G.D. and Brearley, C.A.** (2003) Inositol hexakisphosphate mobilizes an endomembrane store of calcium in guard cells. *Proc. Natl Acad. Sci. U.S.A.* **100**, 10091–10095.
- Levine, T.P. and Munro, S.** (1998) The pleckstrin homology domain of oxysterol-binding protein recognises a determinant specific to Golgi membranes. *Curr. Biol.* **8**, 729–739.

- Levine, T.P. and Munro, S. (2001) Dual targeting of Osh1p, a yeast homologue of oxysterol-binding protein, to both the Golgi and the nucleus–vacuole junction. *Mol. Biol. Cell.* **12**, 1633–1644.
- Levine, T.P. and Munro, S. (2002) Targeting of Golgi-specific pleckstrin homology domains involves both PtdIns 4-kinase-dependent and -independent components. *Curr. Biol.* **12**, 695–704.
- Li, X., Rivas, M.P., Fang, M., Marchena, J., Mehrotra, B., Chaudhary, A., Feng, L., Prestwich, G.D. and Bankaitis, V.A. (2002) Analysis of oxysterol binding protein homologue Kes1p function in regulation of Sec14p-dependent protein transport from the yeast Golgi complex. *J. Cell Biol.* **157**, 63–77.
- Limpens, E., Ramos, J., Franken, C., Raz, V., Compaan, B., Franssen, H., Bisseling, T. and Geurts, R. (2004) RNA interference in *Agrobacterium rhizogenes*-transformed roots of *Arabidopsis* and *Medicago truncatula*. *J. Exp. Bot.* **55**, 983–992.
- Matsuoka, K., Bassham, D.C., Raikhel, N.V. and Nakamura, K. (1995) Different sensitivity to wortmannin of two vacuolar sorting signals indicates the presence of distinct sorting machineries in tobacco cells. *J. Cell Biol.* **130**, 1307–1318.
- McLaughlin, S., Wang, J., Gambhir, A. and Murray, D. (2002) PIP(2) and proteins: interactions, organization, and information flow. *Annu. Rev. Biophys. Biomol. Struct.* **31**, 151–175.
- Meijer, H.J. and Munnik, T. (2003) Phospholipid-based signaling in plants. *Annu. Rev. Plant Biol.* **54**, 265–306.
- Meijer, H.J., Berrie, C.P., Iurisci, C., Divecha, N., Musgrave, A. and Munnik, T. (2001) Identification of a new polyphosphoinositide in plants, phosphatidylinositol 5-monophosphate (PtdIns5P), and its accumulation upon osmotic stress. *Biochem. J.* **360**, 491–498.
- Mirabella, R., Franken, C., van der Krogt, G.N., Bisseling, T. and Geurts, R. (2004) Use of the fluorescent timer DsRED-E5 as reporter to monitor dynamics of gene activity in plants. *Plant Physiol.* **135**, 1879–1887.
- Mueller-Roeber, B. and Pical, C. (2002) Inositol phospholipid metabolism in *Arabidopsis*. Characterized and putative isoforms of inositol phospholipid kinase and phosphoinositide-specific phospholipase C. *Plant Physiol.* **130**, 22–46.
- Munnik, T., Musgrave, A. and de Vrije, T. (1994a) Rapid turnover of polyphosphoinositides in carnation flower petals. *Planta*, **193**, 89–98.
- Munnik, T., Irvine, R.F. and Musgrave, A. (1994b) Rapid turnover of phosphatidylinositol 3-phosphate in the green alga *Chlamydomonas eugametos*: signs of a phosphatidylinositol 3-kinase signalling pathway in lower plants? *Biochem. J.* **298**, 269–273.
- Munnik, T., Irvine, R.F. and Musgrave, A. (1998) Phospholipid signalling in plants. *Biochim. Biophys. Acta.* **1389**, 222–272.
- Odom, A.R., Stahlberg, A., Wente, S.R. and York, J.D. (2000) A role for nuclear inositol 1,4,5-trisphosphate kinase in transcriptional control. *Science*, **287**, 2026–2029.
- Okpodu, C.M., Gross, W., Burkhart, W. and Boss, W.F. (1995) Purification and characterization of a soluble phosphatidylinositol 4-kinase from carrot suspension culture cells. *Plant Physiol.* **107**, 491–500.
- Park, K.Y., Jung, J.Y., Park, J., Hwang, J.U., Kim, Y.W., Hwang, I. and Lee, Y. (2003) A role for phosphatidylinositol 3-phosphate in abscisic acid-induced reactive oxygen species generation in guard cells. *Plant Physiol.* **132**, 92–98.
- Pendaries, C., Tronchere, H., Arbibe, L., Mounier, J., Gozani, O., Cantley, L., Fry, M.J., Gaits-Iacovoni, F., Sansonetti, P.J. and Payrastre, B. (2006) PtdIns(5)P activates the host cell PI3-kinase/Akt pathway during *Shigella flexneri* infection. *EMBO J.* **25**, 1024–1034.
- Perera, N.M., Michell, R.H. and Dove, S.K. (2004) Hypo-osmotic stress activates Plc1p-dependent phosphatidylinositol 4,5-bisphosphate hydrolysis and inositol hexakisphosphate accumulation in yeast. *J. Biol. Chem.* **279**, 5216–5226.
- Preuss, M.L., Schmitz, A.J., Thole, J.M., Bonner, H.K.S., Otegui, M.S. and Nielsen, E. (2006) A role for the RabA4b effector protein PI-4K β 1 in polarized expansion of root hair cells in *Arabidopsis thaliana*. *J. Cell Biol.* **172**, 991–998.
- Ritzenthaler, C., Nebenfuhr, A., Movafeghi, A., Stussi-Garaud, C., Behnia, L., Pimpl, P., Staehelin, L.A. and Robinson, D.G. (2002) Reevaluation of the effects of brefeldin A on plant cells using tobacco Bright Yellow 2 cells expressing Golgi-targeted green fluorescent protein and COPI antisera. *Plant Cell*, **14**, 237–261.
- Roy, A. and Levine, T.P. (2004) Multiple pools of phosphatidylinositol 4-phosphate detected using the pleckstrin homology domain of Osh2p. *J. Biol. Chem.* **279**, 44683–44689.
- Shelton, S.N., Barylko, B., Binns, D.D., Horazdovsky, B.F., Albanesi, J.P. and Goodman, J.M. (2003) *Saccharomyces cerevisiae* contains a type II phosphoinositide 4-kinase. *Biochem. J.* **371**, 533–540.
- Shisheva, A. (2008) PIKfyve: Partners, significance, debates and paradoxes. *Cell Biol. Int.* **32**, 591–604.
- Simonsen, A., Wurmser, A.E., Emr, S.D. and Stenmark, H. (2001) The role of phosphoinositides in membrane transport. *Curr. Opin. Cell Biol.* **13**, 485–492.
- Stenmark, H. and Gillooly, D.J. (2001) Intracellular trafficking and turnover of phosphatidylinositol 3-phosphate. *Semin. Cell Dev. Biol.* **12**, 193–199.
- Stenzel, I., Ischebeck, T., Konig, S., Holubowska, A., Sporysz, M., Hause, B. and Heilmann, I. (2008) The type B phosphatidylinositol-4-phosphate 5-kinase 3 is essential for root hair formation in *Arabidopsis thaliana*. *Plant Cell*, **20**, 124–141.
- Stephens, L., Cooke, F.T., Walters, R., Jackson, T., Volinia, S., Gout, I., Waterfield, M.D. and Hawkins, P.T. (1994) Characterization of a phosphatidylinositol-specific phosphoinositide 3-kinase from mammalian cells. *Curr. Biol.* **4**, 203–214.
- Stevenson, J.M., Perera, I.Y. and Boss, W.F. (1998) A phosphatidylinositol 4-kinase pleckstrin homology domain that binds phosphatidylinositol 4-monophosphate. *J. Biol. Chem.* **273**, 22761–22767.
- Stevenson-Paulik, J., Love, J. and Boss, W.F. (2003) Differential regulation of two *Arabidopsis* type III phosphatidylinositol 4-kinase isoforms. A regulatory role for the pleckstrin homology domain. *Plant Physiol.* **132**, 1053–1064.
- Strahl, T., Hama, H., DeWald, D.B. and Thorner, J. (2005) Yeast phosphatidylinositol 4-kinase, Pik1, has essential roles at the Golgi and in the nucleus. *J. Cell Biol.* **171**, 967–979.
- Thole, J.M., Vermeer, J.E., Zhang, Y., Gadella, T.W. Jr and Nielsen, E. (2008) ROOT HAIR DEFECTIVE4 encodes a phosphatidylinositol-4-phosphate phosphatase required for proper root hair development in *Arabidopsis thaliana*. *Plant Cell*, **20**, 381–395.
- Ueda, T., Uemura, T., Sato, M.H. and Nakano, A. (2004) Functional differentiation of endosomes in *Arabidopsis* cells. *Plant J.* **40**, 783–789.
- Vermeer, J.E.M. (2006) Visualisation of polyphosphoinositide dynamics in living plant cells. PhD thesis, Amsterdam: University of Amsterdam, 178 pp.
- Vermeer, J.E., Van Munster, E.B., Vischer, N.O. and Gadella, T.W. Jr (2004) Probing plasma membrane microdomains in cowpea protoplasts using lipidated GFP-fusion proteins and multimode FRET microscopy. *J. Microsc.* **214**, 190–200.
- Vermeer, J.E., van Leeuwen, W., Tobena-Santamaria, R., Laxalt, A.M., Jones, D.R., Divecha, N., Gadella, T.W. Jr and Munnik, T. (2006) Visualization of PtdIns3P dynamics in living plant cells. *Plant J.* **47**, 687–700.

- Vincent, P., Chua, M., Nogue, F., Fairbrother, A., Mekeel, H., Xu, Y., Allen, N., Bibikova, T.N., Gilroy, S. and Bankaitis, V.A.** (2005) A Sec14p-nodulin domain phosphatidylinositol transfer protein polarizes membrane growth of *Arabidopsis thaliana* root hairs. *J. Cell Biol.* **168**, 801–812.
- Voigt, B., Timmers, A.C., Samaj, J. et al.** (2005) Actin-based motility of endosomes is linked to the polar tip growth of root hairs. *Eur. J. Cell Biol.* **84**, 609–621.
- Walch-Solimena, C. and Novick, P.** (1999) The yeast phosphatidylinositol-4-OH kinase pik1 regulates secretion at the Golgi. *Nature Cell Biol.* **1**, 523–525.
- Weixel, K.M., Blumental-Perry, A., Watkins, S.C., Aridor, M. and Weisz, O.A.** (2005) Distinct Golgi populations of phosphatidylinositol 4-phosphate regulated by phosphatidylinositol 4-kinases. *J. Biol. Chem.* **280**, 10501–10508.
- Wiedemann, C., Schafer, T. and Burger, M.M.** (1996) Chromaffin granule-associated phosphatidylinositol 4-kinase activity is required for stimulated secretion. *EMBO J.* **15**, 2094–2101.
- Yang, W., Burkhart, W., Cavallius, J., Merrick, W.C. and Boss, W.F.** (1993) Purification and characterization of a phosphatidylinositol 4-kinase activator in carrot cells. *J. Biol. Chem.* **268**, 392–398.
- York, J.D., Odom, A.R., Murphy, R., Ives, E.B. and Wente, S.R.** (1999) A phospholipase C-dependent inositol polyphosphate kinase pathway required for efficient messenger RNA export. *Science*, **285**, 96–100.
- York, J.D., Guo, S., Odom, A.R., Spiegelberg, B.D. and Stolz, L.E.** (2001) An expanded view of inositol signaling. *Adv. Enzyme Regul.* **41**, 57–71.
- Zonia, L. and Munnik, T.** (2006) Cracking the green paradigm: functional coding of phosphoinositide signals in plant stress responses. *Subcell. Biochem.* **39**, 207–237.